A Method to Correct the Thermal Dome Effect of Pyranometers in Selected Historical Solar Irradiance Measurements

QIANG JI

Earth System Science Interdisciplinary Center, University of Maryland, College Park, College Park, Maryland

(Manuscript received 21 November 2005, in final form 15 June 2006)

ABSTRACT

In using pyranometers to measure solar irradiance, it is important to know the magnitudes and the consequences of the thermal effect, which is introduced by the glass domes of the instruments. Historically, the thermal dome effect was not monitored on a regular basis. Case studies show that, due to the thermal dome effect, the output of the pyranometers altered from less than 5 W m^{-2} in the nighttime to over 20 W m^{-2} around noontime during the Aerosol Recirculation and Rainfall Experiment (ARREX) in 1999 and the Southern African Fire–Atmosphere Research Initiative (SAFARI) in 2000 field campaigns, depending on sky conditions. A calibration and data processing procedure with the thermal dome effect incorporated has been tested to resolve the issue. It is demonstrated that the intrinsic calibration constants of the pyranometers can be obtained if two pyranometers are used side by side, and the thermal dome effect may be inferred whenever a pyranometer and a pyrgeometer are collocated.

1. Introduction

Climate change–related studies require long-term historical data. One such dataset available and valuable to the climate change community is the solar irradiance measured by the Eppley Precision Spectral Pyranometers (PSPs), which have been populated worldwide (i.e., quantity) for more than three decades (i.e., long term) with very minimal instrumental modifications (i.e., continuity). The double-glass domes of a PSP, acting as both a protector and a filter to the detector, isolate it from convection but alter the radiation balance between the detector and the source of radiation. This introduces the thermal dome effect, which can be quantified by monitoring the variation of temperatures on both the dome and the case of a PSP. The thermal dome effect had been noticed in the early operations of PSPs (e.g., Drummond and Roche 1965), but only began to draw more attention in recent years (e.g., Philipona 2002) due to the quest of better understanding on the so-called cloud absorption anomaly (e.g., Stephens and Tsay 1990). For newer types of pyranometers, such as those manufactured by the Kipp & Zonen (e.g., Model CM21), extraordinary efforts have been devoted to reducing the thermal dome effect. Although a PSP can be modified to infer the thermal dome effect to improve its measurement accuracy (e.g., Bush et al. 2000; Heaffelin et al. 2001), for historical datasets the thermal dome effect was not considered on a regular basis and therefore was buried in the long-term records.

A PSP utilizes a thermopile as the detector, which is assumed to linearly respond to the incoming solar irradiance. Because the dome effect is not considered, the conventional calibration equation for a PSP is simply presenting the irradiance in terms of the output voltage of the thermopile multiplied by a constant calibration factor. Theoretically, a constant intrinsic calibration factor can be used in a calibration equation only when an extra dome effect term is added (Ji and Tsay 2000). Section 2 presents a calibration method to derive the intrinsic calibration factor and to infer the thermal dome effect. Results are shown in section 3 by using measurements acquired during the dry season campaigns of the Aerosol Recirculation and Rainfall Experiment (ARREX) in 1999 and the Southern African Fire–Atmosphere Research Initiative (SAFARI) in 2000. There are some discussions in section 4. The conclusions are presented in section 5.

Corresponding author address: Dr. Qiang Ji, NASA Goddard Space Flight Center, Code 613.2, Greenbelt, MD 20771.
E-mail: ji@climate.gsfc.nasa.gov

DOI:10.1175/JTECH1977.1

© 2007 American Meteorological Society

2. Calibration method

A calibration procedure can be tedious (e.g., Myers et al. 2002; Michalsky et al. 2002), but the basic idea is to measure a known light source and determine a calibration factor. The commonly used calibration equation for pyranometers is

$$I_0 = c_0 V, \tag{1}$$

where I_0 is the derived measurement result, c_0 is the calibration constant, and V is the output voltage of the thermopile. The thermal dome effect is not considered. This will introduce a measurement error, which can be seen in the nighttime as an artificial negative irradiance, or the so-called dark offset or nighttime thermal offset.

To solve the problem, based on analyzing the energy balance of a broadband radiometer (Albrecht and Cox 1974), the idealized calibration equation for a PSP becomes (see Ji and Tsay 2000 for detail):

$$I = cV + D, \tag{2a}$$

where I denotes the incoming solar irradiance; c, the intrinsic calibration constant that depends on the physical properties of the radiometer; and V, the output from the thermopile. The extra term D describes the thermal dome effect of a PSP:

$$D = b\sigma(T_s^4 - T_d^4), \tag{2b}$$

where b represents the dome factor, a constant determined by the ratio of emissivity to transmissivity of the dome; σ, the Stefan–Boltzmann constant; and T_s and T_d, temperatures of the detector and the dome, respectively. Here T_s can be calculated from

$$T_s = T_c + aV, \tag{2c}$$

where T_c is the temperature of the radiometer's case, and $a = 694\ \mathrm{KV}^{-1}$ (Payne and Anderson 1999) for a PSP thermopile. Note, in Eq. (2) only the calibration factor and the thermal dome effect term of a PSP are considered, other effects such as the response of detector to the cosine of the solar zenith angle are not included.

What is the consequence of using Eq. (1)? If the irradiance from the light source during a calibration is kept at I_{cal}, then

$$I_{\mathrm{cal}} = cV_{\mathrm{cal}} + D_{\mathrm{cal}}, \tag{3}$$

where subscript "cal" indicates calibration. Since the dome effect is not measured in a regular PSP, people used to simply ignore D_{cal} and use the following formula to determine a "calibration factor" c_0:

$$I_{\mathrm{cal}} = c_0 V_{\mathrm{cal}}. \tag{4}$$

Note that this formula is accurate only at a single value of known calibration irradiance. By assuming c_0 remains a constant, Eq. (4) is extended to the commonly used Eq. (1). From Eqs. (3) and (4):

$$c = c_0 - D_{\mathrm{cal}}/V_{\mathrm{cal}}. \tag{5}$$

Substitute (5) into (2a):

$$c_0 V = I - D + D_{\mathrm{cal}}/V_{\mathrm{cal}} V. \tag{6}$$

It is clear that $(-D + D_{\mathrm{cal}}/V_{\mathrm{cal}}\, V)$ will be overlooked if Eq. (1) is used.

To use the more accurate equation, (2), the intrinsic calibration constant c and the dome effect D are needed. To determine c, consider two PSPs running side by side; although they have different calibration constants and different dome effect terms, they should report the same irradiance (i.e., $I = c_1 V_1 + D_1 = c_2 V_2 + D_2$). Substitute this into Eq. (6) and a pair of equations are obtained:

$$c_{01} V_1 = c_2 V_2 + (D_2 - D_1 + D_{\mathrm{cal1}}/V_{\mathrm{cal1}} V_1) \quad \text{and}$$

$$c_{02} V_2 = c_1 V_1 + (D_1 - D_2 + D_{\mathrm{cal2}}/V_{\mathrm{cal2}} V_2). \tag{7}$$

The terms on the right-hand side in the parentheses involve the dome effects. As an approximation, a linear fit between (V_2) and $(c_{01} V_1)$ will yield the constant c_2 as the slope of the fitting line, and the average of the remaining dome effect related terms as the intercept. It is similar for c_1.

The dome effect terms cannot be resolved by the PSPs' measurements, so a collocated pyrgeometer is needed. A pyrgeometer is similar to a pyranometer, but measures the infrared irradiance instead. An Eppley Precision Infrared Radiometer (PIR) shares the basic design with PSP but measures the temperatures in the body of the instrument and on the dome for calculating its own thermal dome effect term. When all the radiometers are ventilated and collocated, it is reasonable to assume that the case temperatures of the PSPs and the PIRs should be the same, so the temperature of a PSP's detector, T_s, can be calculated from Eq. (2c).

Because there is no direct measurement of the dome temperature of a PSP, extra assumptions are necessary to retrieve it. At nighttime, the solar irradiance is zero; therefore, Eq. (2a) becomes

$$D = -cV(\text{nighttime}). \tag{8}$$

The $c\ V$, or usually approximated by $c_0 V$ if c is unknown, is the "thermal offset," or the nighttime thermal

dome effect term. PSPs response to the infrared radiation the same way as PIRs do in the nighttime, except with very low efficiency due to the opacity of the domes in infrared. Regarding a PSP as an infrared instrument, the measured infrared irradiance L from the two types of instrument should be identical:

$$L = c_{\mathrm{PIR}}V_{\mathrm{PIR}} + \sigma T_{s\mathrm{PIR}}^4 + b_{\mathrm{PIR}}\sigma(T_{s\mathrm{PIR}}^4 - T_{d\mathrm{PIR}}^4)$$
$$= c_{\mathrm{PSP}}V_{\mathrm{PSP}} + \sigma T_{s\mathrm{PSP}}^4 + b_{\mathrm{PSP}}\sigma(T_{s\mathrm{PSP}}^4 - T_{d\mathrm{PSP}}^4),$$

or

$$c_{\mathrm{PSP}}V_{\mathrm{PSP}} = c_{\mathrm{PIR}}V_{\mathrm{PIR}} + \sigma T_{s\mathrm{PIR}}^4 + b_{\mathrm{PIR}}\sigma(T_{s\mathrm{PIR}}^4 - T_{d\mathrm{PIR}}^4) - \sigma T_{s\mathrm{PSP}}^4 - b_{\mathrm{PSP}}\sigma(T_{s\mathrm{PSP}}^4 - T_{d\mathrm{PSP}}^4).$$

This shows that for infrared the output of a PSP (V_{PSP}) is correlated to the output from a PIR (V_{PIR}) or the "net infrared signal" (e.g., Dutton et al. 2001). The net infrared signal from PIR has been used to infer the thermal response of PSP (Reda et al. 2005); however, to fully explain the thermal offset, the temperatures of the dome and the case of PSP must be captured.

To infer the dome factor of a PSP, a reasonable assumption is that the dome temperature of a PSP is proportional to that of a PIR, because both PSP and PIR are exposed to the same thermal environment:

$$T_d = fT_{d\mathrm{PIR}}(\text{nighttime}), \tag{9}$$

where f is a constant close to unity. Substitute Eqs. (9) and (8) into (2b):

$$-cV/T_{d\mathrm{PIR}}^4/\sigma = bT_s^4/T_{d\mathrm{PIR}}^4 - bf^4(\text{nighttime}). \tag{10}$$

A linear fit between ($T_s^4/T_{d\mathrm{PIR}}^4$) and ($-cV/T_{d\mathrm{PIR}}^4/\sigma$) will give the dome factor b of the PSP as the slope of the fitting line, and bf^4 as the intercept.

Equation (9) is not suitable for the daytime, because the dome temperature is also affected by the solar heating. A natural assumption now is that the outer dome of a PSP will be kept at the case temperature by the ventilation, while the inner dome seeks thermal equilibrium with the outer dome above and the detector surface beneath. Therefore,

$$2\sigma T_{d\mathrm{day}}^4 = \sigma T_c^4 + \sigma T_s^4(\text{daytime}). \tag{11}$$

During the course of a day, the daytime and the nighttime environments dominate alternatively, and the dome temperature switches between $T_{d\mathrm{day}}$ and $T_{d\mathrm{night}}$ gradually. An assumption to incorporate the transition is

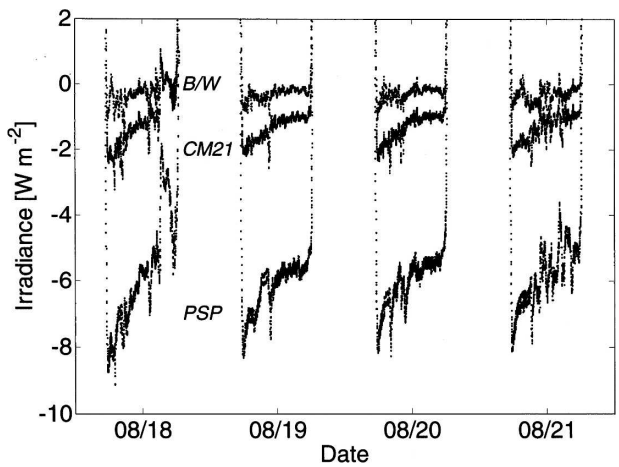

FIG. 1. If the thermal dome effect is ignored in the calibration equation for pyranometers, the effect will show up in the measurement results as an artificial negative irradiance, or the dark thermal offset in the nighttime.

$$T_d = T_{d\mathrm{night}} + T_{d\mathrm{day}} - T_c(\text{daytime and nighttime}). \tag{12}$$

It shows that during the nighttime $T_{d\mathrm{day}}$ approaches T_c because of the lack of solar hearting, so $T_{d\mathrm{night}}$ dominates; therefore, during the daytime, since $T_{d\mathrm{night}}$ almost equals $T_{d\mathrm{PIR}}$, which closely follows T_c, $T_{d\mathrm{day}}$ dominates.

With all necessary parameters determined, Eq. (2) with the thermal dome effect considered, instead of the simplified Eq. (1), can be applied to a PSP.

3. Data and results

During the dry season campaign of the ARREX in August 1999, a group of radiometers were deployed at the airport at Skukuza in South Africa. Among other sensors, there were two PSPs (SN: 32107, 32188), a couple of PIRs (SN: 32193, 32194), a pair of Kipp & Zonen CM21s (SN: 980563, 980564), and an Eppley Black-and-White (B/W, SN: 21563). They were calibrated at the National Oceanic and Atmospheric Administration/National Renewable Energy Laboratory (NOAA/NREL) in July 1999. Clear domes were installed on all of the pyranometers from 17 to 21 August 1999.

Figure 1 shows the "dark offsets" caused by using Eq. (1). As expected, the B/W has little offset because the thermal dome effect is cancelled by design, the CM21s have small offsets of less than 2 W m^{-2}, while PSPs have larger offsets ranging from 5 to beyond 8 W m^{-2}. This implies that the CM21s perform better than the PSPs in term of dealing with thermal dome effect, but it is not fully compensated as the B/W.

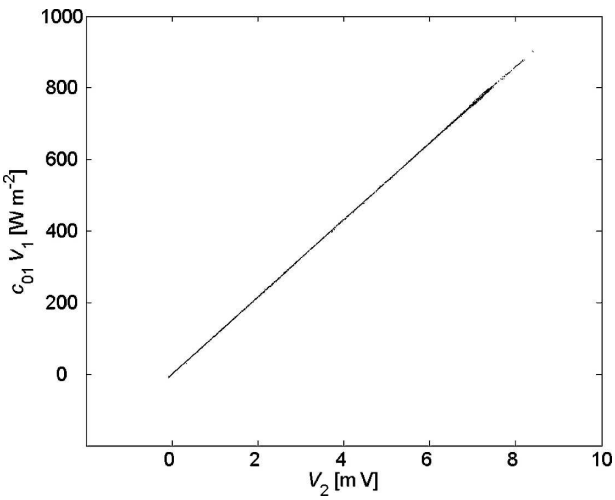

FIG. 2. The "measurement result" from the first PSP with the dome effect ignored is almost linearly related to the output of the thermopile from the second one. The slope of the fitting line will be regarded as the intrinsic calibration constant for the second PSP.

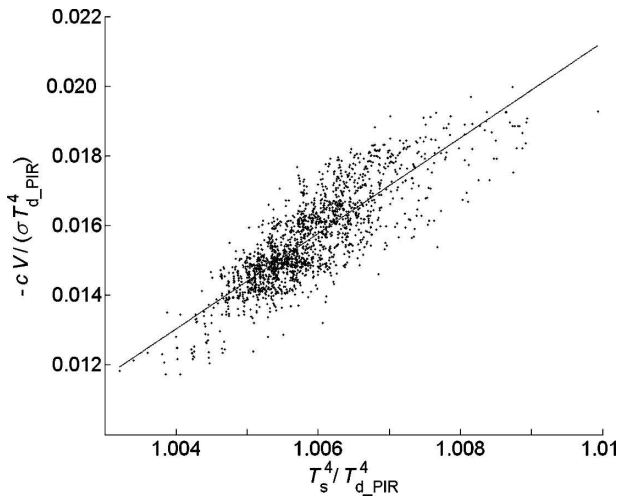

FIG. 3. This scatterplot and linear fitting line is made for PSP 32188 from 4 days of nighttime data (after 8 P.M. and before 4 A.M. next morning local time). The slope of the fitting line will be regarded as the dome factor for this PSP.

Figure 2 is the scatterplot of the output voltage from PSP 32188 versus the calculated irradiance from PSP 32107 excluding the dome term. The calibration factor is c_{01} = 114.36 W m^{-2} mV^{-1} for PSP 32107, and c_{02} = 108.19 W m^{-2} mV^{-1} for PSP 32188. After a linear fit, the estimated intrinsic calibration constant is c_1 = 114.87 W m^{-2} mV^{-1} for PSP 32107 (see more explanations in the discussion section), and c_2 = 107.71 W m^{-2} mV^{-1} for PSP 32188.

As shown in Fig. 3, with the newly determined intrinsic calibration constants, Eq. (10) is used to infer the dome factors and dome temperatures. The results are b = 1.30, f = 0.9983 for PSP 32107, and b = 1.37, f = 0.9986 for PSP 32188. Notice that f is slightly smaller than 1, which is consistent with the emissivity of the PSP's glass dome being larger than the PIR's silicon dome. Therefore, while exposed to the cold sky in nighttime, the dome temperature of PSP should be lower than that of PIR.

To reveal the transition of dome temperature due to the daytime and nighttime energy balances in a PSP, a day of dome temperature from PSP 32188, subtracting T_s for better viewing, is shown in Fig. 4. Accordingly, the calculated thermal dome effect term can be found in Fig. 5, which gives the details on how the dome effect of the PSP changed from 5 to ~8 W m^{-2} during the nighttime to over 20 W m^{-2} around noontime. Also shown is an estimation of the thermal dome effect of a CM21, which is treated the same as a PSP for demonstration. CM21s have a smaller dome effect due to the better thermal contact between their domes and their cases, plus other improvements. However, the negative output in the nighttime shows that the thermal dome effect still physically exists.

Finally, the corrected irradiance can be obtained by using Eq. (2a). Figure 6 is an example of the results. It highlights that by using the calibration equation with the dome effect included (solid curves in the figure), the measurement results from all the radiometers become more consistent, and the artificial negative irradiance during the nighttime is eliminated.

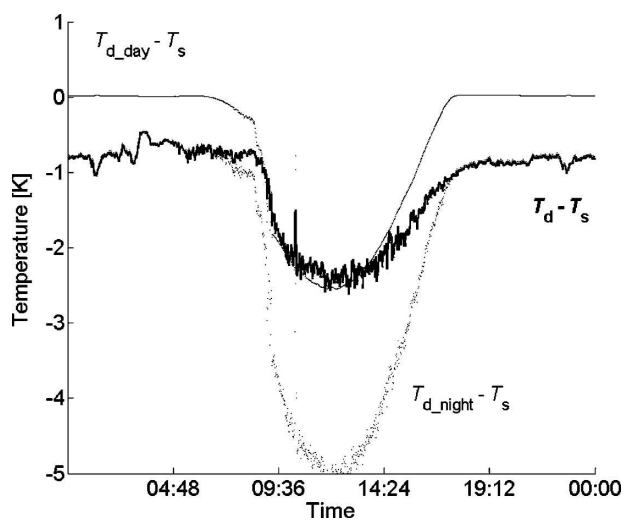

FIG. 4. The dome temperature of PSP 32188 on 18 Aug 1999; T_s is subtracted for better viewing. The thick curve shows how T_d shifts between $T_{d\text{night}}$ (lower dotted curve) and $T_{d\text{day}}$ (upper curve).

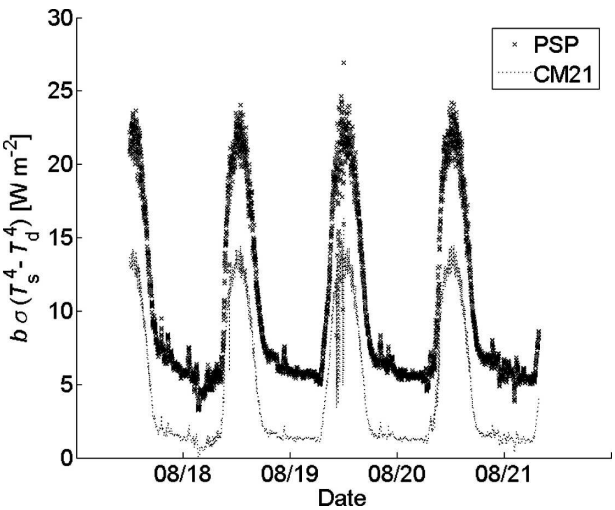

FIG. 5. The calculated thermal dome effect. Collocated CM21s have a smaller dome effect than the PSPs.

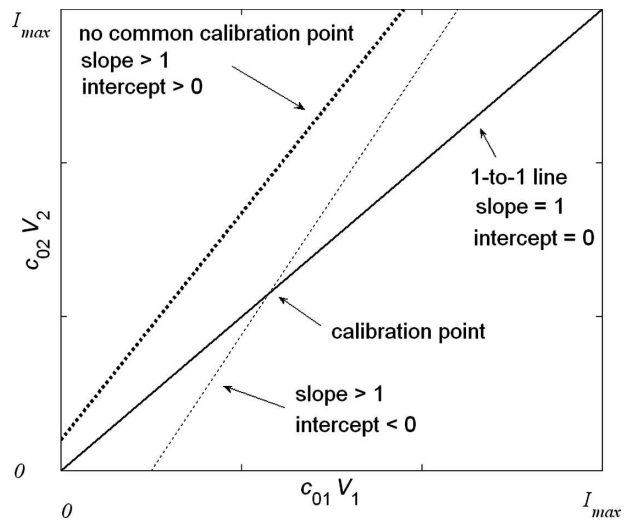

FIG. 7. This conceptual plot illustrates the relationship between the measurements from two PSPs. The I_{max} is the range of measurement. The ($c_{01}V_1$) versus ($c_{02}V_2$) plot is expected to meet the one-to-one line at the calibration point. When they do not meet, the PSPs have not been calibrated under the same irradiance with I_{max}.

4. Discussion

a. Calibration point

According to Eq. (5), c is expected to be smaller than c_0 for a PSP. However, the result for PSP 32107 shows the opposite in the case study. A possible explanation is related to an inconsistency of c_0, which may be because the two PSPs were not calibrated under the same irradiance. Figure 7 illustrates the concept. Ideally, if both PSPs were identical and calibrated without uncertainties, then the relationship of irradiances [i.e., (c_{01} V_1) versus (c_{02} V_2)], would follow the one-to-one line. If the two PSPs are not identical, then it is expected that the relationship will follow a line that meets the one-to-one line at the irradiance where they were calibrated together (i.e., the "calibration point"). In other words, the fitting line will have either a larger-than-unity slope with a negative intercept (thin dotted line in the figure) or a smaller-than-unity slope with a positive intercept (not shown in the figure). The data in the case study follows a larger-than-unity slope (1.004) with a positive intercept (0.13) for PSP 32107 versus PSP 32188, which implies that the two PSPs do not have a common calibration point in the measured range of irradiance. Relatively c_0 is underestimated for PSP 32107. Follow the set of Eqs. (7), (2a), and (10), if c_0 is underestimated, then c will become larger to compensate.

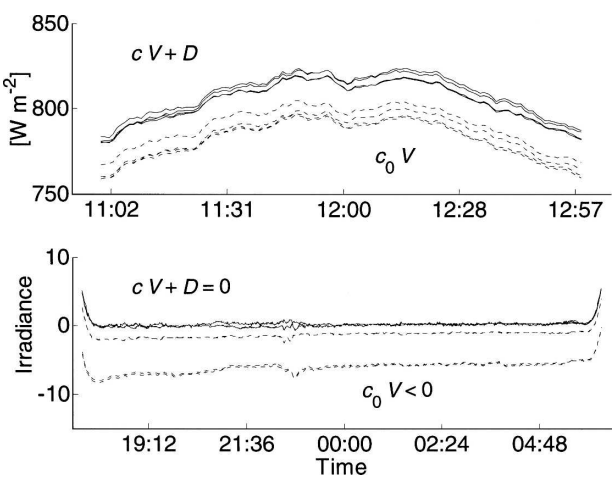

FIG. 6. Irradiance measured by the two PSPs and the two CM21s on 18 Aug 1999: (top) 2 h around noontime and (bottom) the whole night. The solid curves are with the thermal dome effect considered ($cV + D$), while the dotted curves are without (c_0V).

The inconsistency of c_0 is either because they were not calibrated together or because of the statistical nature of the calibration procedure. For example, if the PSPs were not calibrated under a particular irradiance, but were put in the field and the calibration factors were found statistically during the course of a day, then it may yield an equivalent calibration point for each PSP, but does not guarantee a common calibration point for all the PSPs.

For a given pyranometer, Eqs. (1) and (2) should report the correct irradiance at the calibration point (i.e., $I_{cal} = c_0V_{cal} = cV_{cal} + D_{cal}$). As shown in Fig. 8, which is based on real data but exaggerated in the plot, because Eq. (2) correctly reports zero solar irradiance in the nighttime but Eq. (1) always gives a negative value, Eq. (1) tends to underestimate irradiance bellow

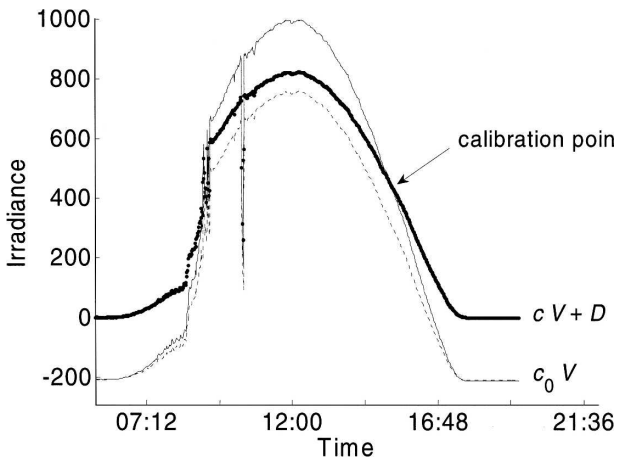

FIG. 8. This conceptual plot (based on 18 Aug 1999 data) illustrates the calibration point where $I_{cal} = c_0V_{cal} = cV_{cal} + D_{cal}$. The dotted curve shows the case of lack of a calibration point due to either the relative underestimation of c_0, or overestimation of c and/or D, or the calibration point is above the measured range of irradiance.

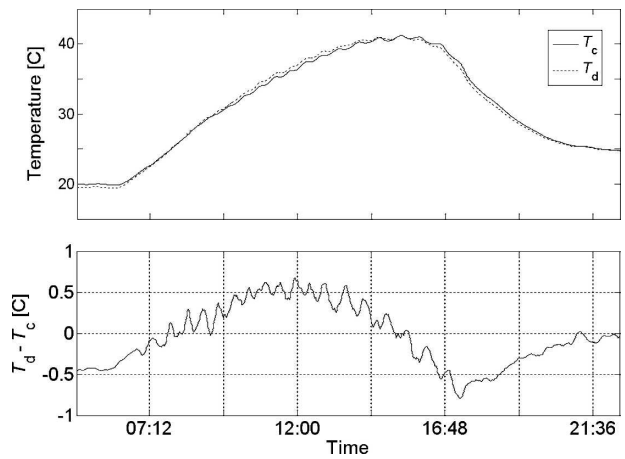

FIG. 9. (top) Dome (T_d) and case (T_c) temperatures of a PIR and (bottom) their difference on 13 Sep 2000 during the SAFARI 2000 field experiment. The ripples are cause by turning the ventilation on and off.

the calibration point (when $I < I_{cal}$), and overestimate above the calibration point (when $I > I_{cal}$). In the case study, the irradiance from Eq. (1) is smaller than from Eq. (2) for the whole range of measurement, as illustrated by the dotted curve and the thick curve in Fig. 8. This leads to several possibilities: 1) the calibration point is above the range of measurement; 2) c_0 is underestimated; and/or 3) either c or D, or both, is overestimated. This requires further investigation because of all the assumptions involved. The question may be answered if D is directly measured.

b. Effect of ventilation

To study the thermal dome effect, a test was performed on 13 September 2000 during the SAFARI 2000 field experiment at the same site as during the ARREX 1999. It was a cloud-free day, and the air temperature reached 35°C in the early afternoon. Figure 9 shows the temperatures of the dome and the case temperatures of a PIR. The ripples in the curves are related to the ventilation. The ventilators of the PIR and a PSP were on before dawn; they were turned off and on alternatively every 15 min in the morning, and every 20 min in the afternoon; they were left off in the evening. The ventilation tended to bring the temperature of the instruments close to the air temperature. As a result, during the daytime, it cooled the dome and the case, but cooled the case more than the dome; during the nighttime, it warmed the dome and the case, but warmed the case more than the dome. Therefore, as shown in Fig. 10, the magnitude of the thermal dome effect of the PIR that is calculated from Eq. (2b), became larger whenever it was ventilated. Notice that the ventilation does not affect the measurement result of the infrared irradiance, because the thermal dome effect is considered in the calibration equation for a PIR. However, the PSP's measurement result is affected if Eq. (1) is used. The curve in the middle of Fig. 10 is from the PSP's output, normalized to another PSP that was con-

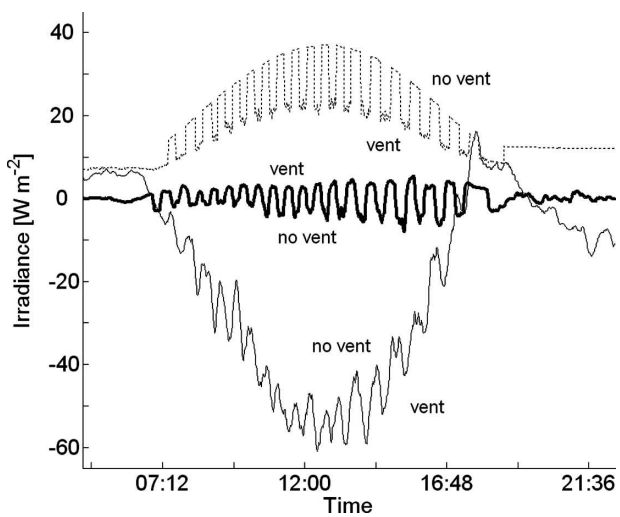

FIG. 10. On 13 Sep 2000, the ventilations of a PIR and a PSP were turned off and on alternatively during the course of the day. The thick curve in the middle is the PSP's output normalized to another PSP that was constantly ventilated. It shows that the output will drop due to the thermal dome effect whenever the ventilation is off. The lower curve is the dome effect of the PIR, which is negative because the infrared radiation is outgoing into the sky during the daytime. The dotted curve at the top illustrates the estimated dome effect of the PSP.

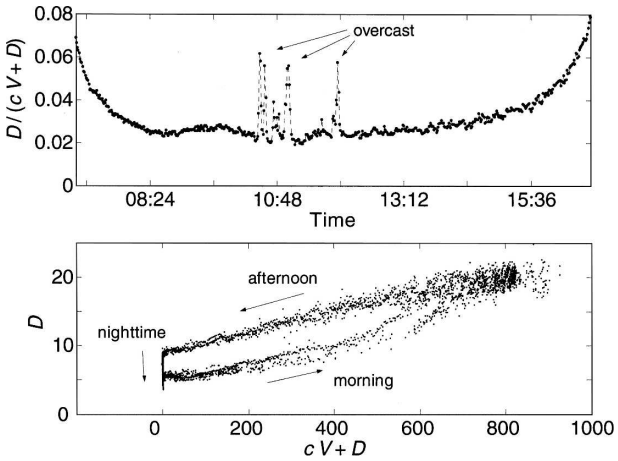

FIG. 11. (top) The ratio of the dome effect term to the irradiance, which decreased during the daytime on 19 Aug 1999. The ratio increased during several overcast periods around noontime. (bottom) The relationship between the thermal dome effect term and the irradiance. The pattern followed the daily air temperature.

stantly ventilated. Whenever the PSP's ventilation was off, the output of the thermopile decreased. This is the response, which is predicted by Eq. (2), to the larger thermal dome effect introduced by the greater temperature difference between the dome and the case. The calculated dome effect of the PSP is shown in Fig. 10 at the top (dotted curve). For the unventilated period, the dome temperature is unknown, so Eq. (11) is modified by assuming the outer dome of the PSP reached thermal balance between the detector and the cold sky, and 4% of the infrared energy from the sky measured by the PIR is added to match the more than 13 W m^{-2} dark thermal offset.

Reversing ventilation airflow, so it went through the dome first, reduced the temperature discrepancy between the dome and the case, although it did not affect the measurement result of a PIR. To reduce thermal dome effect, the 115-VAC fans in the Epply ventilators used during the SAFARI 2000 were replaced by some compatible 12-VDC fans after the field campaign.

c. Consequence of ignoring thermal dome effect

Figure 11 shows the ratio between the dome effect and irradiance, $D/(c\,V + D)$, from 19 August 1999 during ARREX. The diurnal change of the ratio followed the change of the air temperature. The ratio decreased to about 2.5% around noontime when the irradiance reached about 900 W m^{-2}. Notice that there are a few cases in which the ratio increased to about 6%. Those are cloudy periods when the irradiance dropped to about 200 W m^{-2}.

What is the significance of a changing ratio? Hypothetically, imagine using a PSP to measure solar irradiance in the atmosphere. First, assume the downward irradiance above a scattering layer is 800 W m^{-2}, and the underestimation by ignoring the thermal dome effect is 20 W m^{-2}, so the measurement becomes 780 W m^{-2}. Second, assume the downward irradiance below the layer is 400 W m^{-2}, and the underestimation by ignoring the thermal dome effect, now smaller but at a higher ratio, is 15 W m^{-2}, so the measurement is 385 W m^{-2}. Third, assume there is no absorption and the ground surface is dark, then the upward irradiance above the layer due to the reflection has to be 400 W m^{-2}; with the 15 W m^{-2} underestimation, the measurement will be 385 W m^{-2} again. Now consider the energy balance. Apparently 780 W m^{-2} goes into the scattering layer, but 385 + 385 = 770 W m^{-2} comes out; 10 W m^{-2} are missing. The result will be the same if the radiometer overestimates irradiance instead of underestimating it.

Also hypothetically when the upward irradiance is measured, the pyranometer will look toward a warmer ground surface instead of a colder sky. A discrepancy due to the different thermal backgrounds can occur if the thermal effect is ignored.

Generally, as long as the thermal dome effect has been involved in calibrations or in measurements, certain degrees of "abnormal" can be introduced.

5. Conclusions

In conclusion, the thermal dome effect of a pyranometer is overlooked in the commonly used and simplified calibration equation, which is equivalent to regarding a varying calibration factor as a constant. The result is that a pyranometer can artificially underestimates the solar irradiance by a few percent. After analyzing the energy balance in a pyranometer and deriving its less simplified calibration equation that includes the thermal dome effect, it is believed that the thermal dome effect of the Eppley PSP broadband radiometer (pyranometer) can be estimated, and the long-term historical measurements of PSPs can be corrected if a PIR were collocated. The intrinsic calibration constant can also be determined when two PSPs are used side by side. The major assumptions are the following: 1) with ventilations, the case temperatures of the collocated instruments remain identical; 2) the nighttime dome temperature of a PSP is proportional to that of the PIR; 3) the daytime dome temperature of the PSPs is controlled by the thermal balance of the sensor and the case temperatures of the instrument; and 4) the dome temperature changes gradually between the daytime

and nighttime according to Eq. (12). The field experiment data from ARREX 1999 and SAFARI 2000 show that the method works effectively; the underestimations of irradiance are compensated, and the artificial nighttime offsets are eliminated.

For future work, the assumptions may be refined, and the accuracy of the method can be investigated by using a modified pyranometer with the dome and the case temperatures monitored. Reprocessed historical data and the new measurements with the thermal dome effect considered will play important roles in climate studies.

Acknowledgments. This study was supported by NASA's Radiation Science Program, managed by Dr. Robert J. Curran. Field campaigns were also supported by ONR's Marine Meteorology Program, managed by Dr. Ronald J. Ferek. Special thanks are due to Dr. Tom Stoffel and his group at NOAA/National Renewable Energy Laboratory for calibrating our radiometers; to Dr. Stuart J. Piketh of the Climatology Research Group, University of Witwatersrand, South Africa, for help during the field campaigns; and to Dr. Si-Chee Tsay at NASA Goddard Flight Center for support and suggestions.

REFERENCES

Albrecht, B. A., and S. K. Cox, 1974: Pyrgeometer measurements from aircraft. *Rev. Sci. Instrum.,* **45,** 33–38.

Bush, B. C., F. P. J. Valero, A. S. Simpson, and L. Bignone, 2000: Characterization of thermal effects in pyranometers: A data correction algorithm for improved measurement of surface insolation. *J. Atmos. Oceanic Technol.,* **17,** 165–175.

Drummond, A. J., and J. J. Roche, 1965: Corrections to be applied to measurements made with Eppley (and other) spectral radiometers when used with Schott colored glass filters. *J. Appl. Meteor.,* **4,** 741–744.

Dutton, E. G., J. J. Michalsky, T. Stoffel, B. W. Forgan, J. Hickey, D. W. Nelson, T. L. Alberta, and I. Reda, 2001: Measurements of broadband diffuse solar irradiance using current commercial instrumentation with a correction for thermal offset errors. *J. Atmos. Oceanic Technol.,* **18,** 297–314.

Heaffelin, M., S. Kato, A. M. Smith, C. K. Rutledge, T. P. Charlock, and J. R. Mahan, 2001: Determination of the thermal offset of the Eppley precision spectral pyranometer. *Appl. Opt.,* **40,** 472–484.

Ji, Q., and S.-C. Tsay, 2000: On the dome effect of Eppely pyrgeometers and pyranometers. *Geophys. Res. Lett.,* **27,** 971–974.

Michalsky, J., and Coauthors, 2002: Broadband shortwave calibration results from the Atmospheric Radiation Measurement Enhanced Shortwave Experiment II. *J. Geophys. Res.,* **107,** 4287, doi:10.1029/2001JD001231.

Myers, D. R., T. L. Stoffel, I. Reda, S. M. Wilcox, and A. M. Andreas, 2002: Recent progress in reducing the uncertainty in and improving pyranometer calibrations. *J. Sol. Energy Eng.,* **124,** 44–50.

Payne, R. E., and S. P. Anderson, 1999: A new look at calibration and use of Eppley Precision Infrared Radiometers. Part II: Calibration and use of the Woods Hole Oceanographic Institution Improved Meteorology Precision Infrared Radiometer. *J. Atmos. Oceanic Technol.,* **16,** 739–751.

Philipona, R., 2002: Underestimation of solar global and diffuse radiation measured at Earth's surface. *J. Geophys. Res.,* **107,** 4654, doi:10.1029/2002JD002396.

Reda, I., and Coauthors, 2005: Using a blackbody to calculate net longwave responsivity of shortwave solar pyranometers to correct for their thermal offset error during outdoor calibration using the component sum method. *J. Atmos. Oceanic Technol.,* **22,** 1531–1540.

Stephens, G. L., and S.-C. Tsay, 1990: On the cloud absorption anomaly. *Quart. J. Roy. Meteor. Soc.,* **116,** 671–704.